Structure and dynamics of amorphous water ice

D. Laufer, E. Kochavi, and A. Bar-Nun
Department of Geophysics and Planetary Sciences, Tel Aviv University, Ramat Aviv, 69978, Tel Aviv, Israel
(Received 18 May 1987)

Further insight into the structure and dynamics of amorphous water ice, at low temperatures, was obtained by trapping in it Ar, Ne, H_2, and D_2. Ballistic water-vapor deposition results in the growth of smooth, $\sim 1 \times 0.2$ μm^2, ice needles. The amorphous ice seems to exist in at least two separate forms, at $T < 85$ K and at $85 < T < 136.8$ K, and transforms irreversibly from one form to the other through a series of temperature-dependent metastable states. The channels formed by the water hexagons in the ice are wide enough to allow the free penetration of H_2 and D_2 into the ice matrix even in the relatively compact cubic ice, resulting in H_2- (D_2-) to-ice ratios (by number) as high as 0.63. The larger Ar atoms can penetrate only into the wider channels of amorphous ice, and Ne is an intermediate case. Dynamic percolation behavior explains the emergence of Ar and Ne (but not H_2 and D_2) from the ice, upon warming, in small and big gas jets. The big jets, each containing $\sim 5 \times 10^{10}$ atoms, break and propel the ice needles. Dynamic percolation also explains the collapse of the ice matrix under bombardment by Ar, at a pressure exceeding 2.6 dyn cm^{-2}, and the burial of huge amounts of gas inside the collapsed matrix, up to an Ar-to-ice ratio of 3.3 (by number). The experimental results could be relevant to comets, icy satellites, and icy grain mantles in dense interstellar clouds.

I. INTRODUCTION

The very high capacity of amorphous water ice at low temperatures for trapping various gases (Ar, CO, CH_4, N_2), was recently reported by us.[1,2] It was shown that the amount of internally trapped gas can be as high as 3.3–3.5 times the amount of the ice itself. The single mechanism by which the ice traps the gas was found to be the slow, temperature dependent creeping and annealing of the amorphous ice, which seals the gas in it. Upon warming, each one of these gases is released from the ice in eight distinct temperature ranges [Fig. 1(a)], starting at (*a*) 23 K, where the frozen excess gas, which was not trapped internally, evaporates; (*b*) 35 K, where the slow annealing of the ice releases some of the trapped gas; (*c*) 44 K, where the monolayer of adsorbed gas evaporates from the 86 $m^2 g^{-1}$ surface of the ice; (*d*) 85 K, where the slow annealing of the ice, up to 120 K, releases some additional gas; (*d'*) 122 K, which might be associated with a glass transition in the amorphous ice; (*e*) 136.8 K, during the transformation of the amorphous ice into cubic ice, when the ice matrix softens temporarily, letting out some of the trapped gas; (*f*) 160.0 K, during the transformation of the cubic ice into hexagonal ice; and finally, (*g*) at ~ 180 K, where the ice itself evaporates, releasing the gas which was trapped in the clathrate-hydrate cages.

From this description, it is clear that all the processes of gas release, except the first one, are a result of the dynamics of the ice itself, and the release of the gas is merely a manifestation of the changes in the ice. Thus the dynamic range of gas detection by a quadrupole mass filter, which spans 10 orders of magnitude, enables the detection of very subtle changes in the ice.

In order to obtain a better insight into the structure and dynamics of the ice, we extended the study to include smaller gases, such as hydrogen, deuterium, and neon. The trapping of these gases was already studied to some extent,[3–5] but the amounts trapped were orders of magnitude smaller than those found by us with argon, methane, nitrogen, and carbon monoxide. In addition, we studied in greater detail the previously reported[1,2] ejection of gas jets and ice grains, which accompany the gas release.

The new experimental results, together with the application of dynamic percolation theory, extended considerably our understanding of the processes ocurring in the ice, the mechanism by which it traps such large amounts of gas, and how this gas is released from the ice. Such understanding is essential for a well-founded physical description of the processes which take place in the icy bodies of the solar system and the dense interstellar clouds.

II. EXPERIMENT PROCEDURE

The experimental setup and procedures were described in detail in our previous papers[1,2] and will therefore be described here only briefly. The test chamber and its pump consisted of two 10-in. cryogenic pumps, connected head to head by a 6-in. gate valve. After rough pumping the chamber to 10^{-4} Torr by a sorption pump, the pressure in it was lowered to better than 10^{-8} Torr by the cryogenic pump. A thick, 5×2.5 cm^2, gold-coated copper plate was cooled cryogenically (by the chamber's cold finger) to ~ 20 K, and its temperature could be controlled by heating, between 20 and 250 K, within ± 2 K. A stream of water vapor, from a reservoir of thoroughly degassed triply distilled water, was directed at the plate through a capillary tubing with a diffuser

on its tip. A layer of ice, containing $10^{19}-10^{20}$ water molecules, was deposited on the plate during 5–45 min. A stream of argon (Matheson Research Grade, 99.995% pure) was then directed at the ice, through the same capillary tubing, at 20–150 K and pressures of 8×10^{-4}–0.1 Torr for 5–45 min, keeping the gate valve fully open. Alternatively, a premixed argon–water-vapor mixture was flowed onto the cold plate and was co-deposited on it. When the deposition was terminated, the chamber was pumped for ~10 min, until a constant pressure of $\sim10^{-8}$ Torr was reached. The plate was then uniformly warmed, at a constant rate of 0.1–3 K min^{-1}. The trapping of neon, hydrogen, and deuterium (Matheson Research Grade, 99.995% pure) was studied at 15–25 K on the cold finger itself, and its warming, at a rate of 4 K min^{-1}, was achieved by

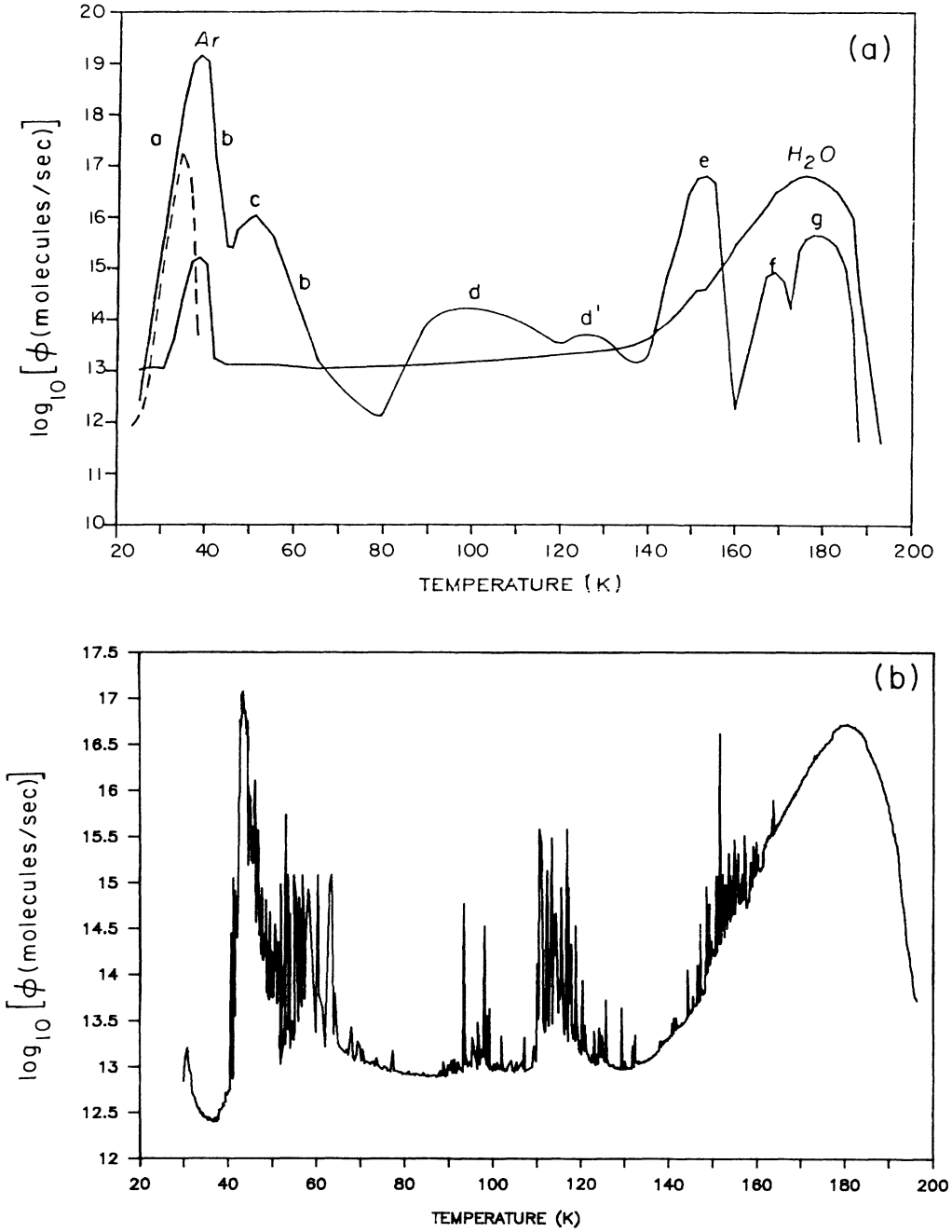

FIG. 1. (a) A plot of the fluxes (ϕ) of evolved argon and water vs temperature, representing the *eight* ranges of gas evolution. The fluxes vary by up to 8 orders of magnitude as the ice temperature varies. The rise in the water flux at 30 K is due to ice-grain ejection. An evaporation curve of frozen argon from an ice-free plate (— — —) is added for comparison. (b) A plot of the fluxes (ϕ) of water vs temperature, from a co-deposition of a 1:1 Ar-H_2O mixture at 25 K, showing the ranges of ice-grain ejection. The time scale in this measurement did not allow the separation of single grains, which was shown earlier (Ref. 2).

switching off the cold head. The evolution of gas and water vapor from the ice was monitored by a precalibrated quadrupole mass-filter and the amounts of gas and water vapor emerging at each temperature range were obtained by integrating their fluxes over the time of their evolution from the ice.

During the evolution of gas at the various temperature ranges, spikes of water and argon were monitored by the quadrupole mass filter. Each spike corresponds to an argon jet or to an ice grain, which enter the mass filter's probe. From the area under each spike, the amounts of water and argon could be calculated, taking into account the different geometries for sampling a jet or an ice grain entering the probe, as compared with the sampling of a uniform cloud of gas or water vapor emanating from the sample plate.

III. RESULTS AND DISCUSSION

A. The structure of the amorphous ice

When a layer of gas-free amorphous ice is viewed from the edge or at an oblique angle, a hairlike structure is revealed (Fig. 2). The ice looks like a shaggy woolen carpet, which explains the very large surface area (86 $m^2 g^{-1}$) reported earlier.[2] The separate needles are seen to be growing when additional amounts of water vapor are frozen on the plate. Needles about 0.1 mm long are seen in Fig. 2, where a hundredfold more ice than usual was deposited on the plate. The amorphous ice needles, which grow by ballistic deposition of water vapor, are smooth, with no side branches,[6] unlike the dendritic structure of hexagonal ice, which grows on a cold surface by diffusion of water vapor in air.[7] The same structure is formed with water deposition rates between 10^{17} and 10^{19} water molecules/cm^2 min, at temperatures between 20 and 100 K. The ice needles are not altered during the evaporation of the ice between ~ 140 and ~ 180 K and retain their shape until their complete evaporation. Since the observation of the needles is merely visual, it is not clear whether submicrometer ice layers also have the same appearance. If a needlelike growth begins from the plate's surface, the ice density of ~ 0.65 g cm^{-3} which was measured by us previously, by interference rings from submicrometer ice layers,[2] has no physical meaning.

B. Ice grains and gas jets

Very large fluxes of gas jets, each containing about 5×10^{10} gas molecules, and ice grains, each containing about 10^{10} water molecules, are emitted from the ice under a variety of conditions [Fig. 1(b)]: (1) whenever Ar, CO, CH_4, N_2, and Ne, but not H_2 or D_2, are emitted from gas-rich ice; (2) during the deposition of a 1:1 gas–water-vapor mixture below 29 K; and (3) during gas flow into pure amorphous ice, below 29 K; at a pressure exceeding 2.6 dyn cm^{-2}.

In addition to the large gas jets, all gas emission in the various ranges is not quiescent, but consists of numerous minijets, ~ 100 times smaller than the large ones, which result in a "noisy" gas signal at a frequency of $\sim 10^3$

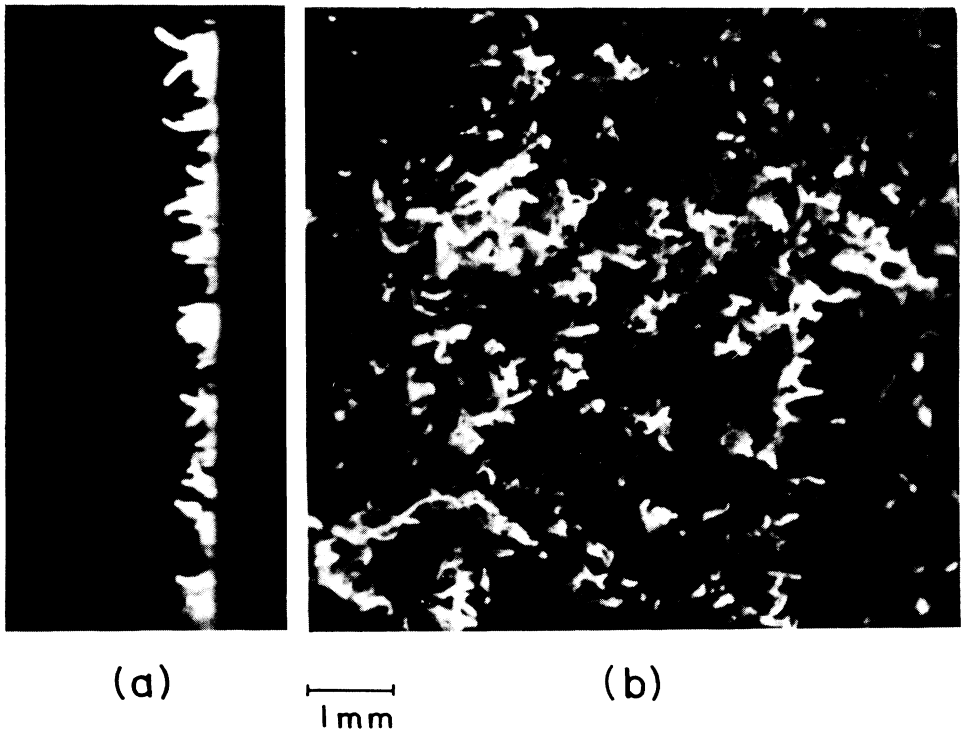

FIG. 2. Two views of an amorphous ice layer, seen edge-on (a) and at an oblique angle (b), both magnified 15 times. Needles about 0.1 mm long are seen, with an ice layer containing $\sim 10^{20}$ water molecules/cm^2.

sec^{-1}. Thus the large gas jets are superimposed on a continuous stream of smaller gas jets. The relative amount of gas which is emitted in the large jets, as compared with the small ones, is proportional to the total amount of gas stored in the ice.

Whenever a large flux of ice grains is emitted, the ice remaining on the plate is not hairlike, but has a very rough texture. Therefore it seems that the ice grains are indeed the ice needles, which are broken from their base and are propelled by the large gas jets. The ejection of the needles is also correlated with the amount of gas trapped in the ice, as demonstrated by the following two experiments. A 1:1 argon-water vapor mixture was deposited on the plate at 25 and 50 K. At 25 K, a large flux of ice needles was observed during the deposition, and the remaining ice was rough but needleless. However, at 50 K, no needles were ejected and the ice was hairlike. The argon-to-ice ratio at the end of the deposition was 10 times larger at 25 K than at 50 K.

The amount of ice in the ejected needles is larger than both the amount of gas trapped in them and the amount of gas in the jets which propel them. This can be seen from the enhancement, by up to a factor of 10, in the gas-to-ice ratio after a large flux of ice needles. This behavior was studied in detail by depositing various amounts of pure water vapor, pure argon, and mixtures of the two, and also by flowing various amounts of argon into pure water ice, all at several temperatures between 25 and 50 K. The results are shown in Fig. 3. Of all the variables in these experiments, the only parameter which affects the amount of ice remaining on the plate is the amount of trapped gas. Large amounts of trapped gas lower the amount of ice by up to a factor of 4. Thus, four times more ice can be lost by the ejection of ice needles than the amount remaining on the plate. This could perhaps represent the ratio between the amounts of ice in the needles and in the rough ice which is left on the plate, unless the rough ice itself is formed by the collapse of ice needles and their sticking together. The enhancement by up to a factor of 10 in the gas-to-ice ratio, after heavy needle-ejection, is thus explained by a fourfold lowering of the amount of ice and the steeper curve of growth of frozen argon than that of pure water ice, as seen in Fig. 3.

Analysis of several hundred ice needles and large gas jets, which were emitted between 36 and 39 K, yields the histograms shown in Fig. 4. The distribution of both ice needles and argon jets is nearly Gaussian and quite narrow, with 84% of the needles containing between 3×10^{9} and 3×10^{10} water molecules and 86% of the jets containing between 10^{10} and 10^{11} argon atoms. The narrow ice distribution suggests that the ice needles grow at a nearly uniform rate and reach a nearly uniform size. The narrow gas distribution suggests that the large jets are formed whenever a critical gas concentration is reached.

The ratio of the needles' length to their diameter is, from Fig. 2, about 5. Hence, 10^{10} water molecules in an

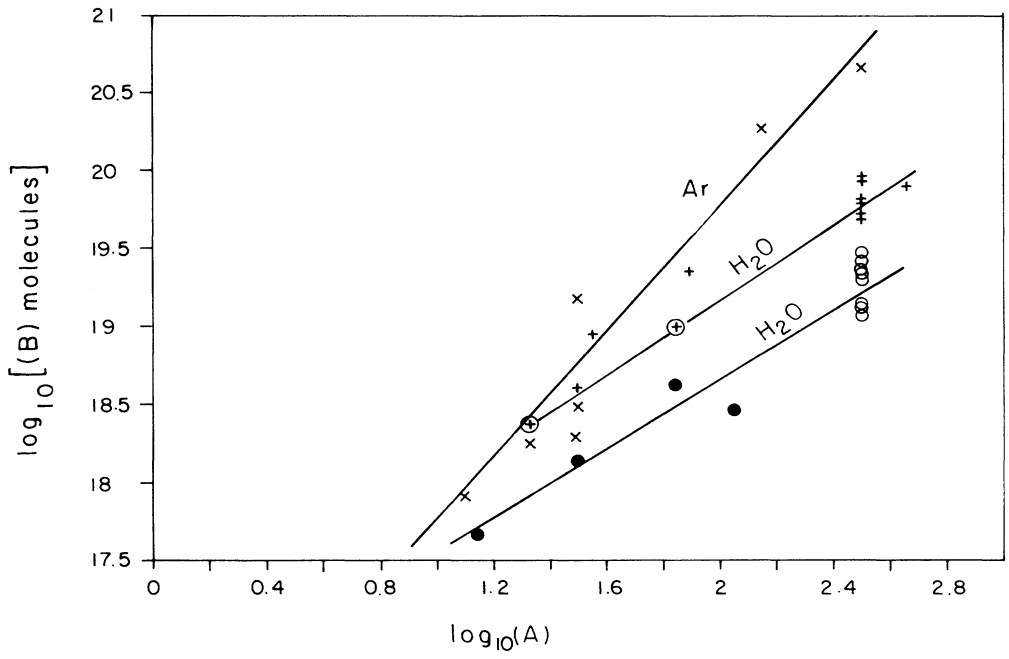

FIG. 3. The amounts of water or argon remaining on the plate (B) vs the relative amounts of water or argon which were flowed onto the plate (A). ●, co-deposition of a 1:1 Ar-H_2O mixture at 25 K; ○, Ar flowed into water ice at 25 K; +, co-deposition of a 1:1 Ar-H_2O mixture and Ar flow into ice, both at 50 K; ⊕, deposition of pure water at 25 K; ×, deposition of Ar on a water-free plate at 25 K. Two distinct lines are seen for the amount of ice—one with a lot of trapped gas and the other with little or no gas. Note also the steeper curve for frozen argon.

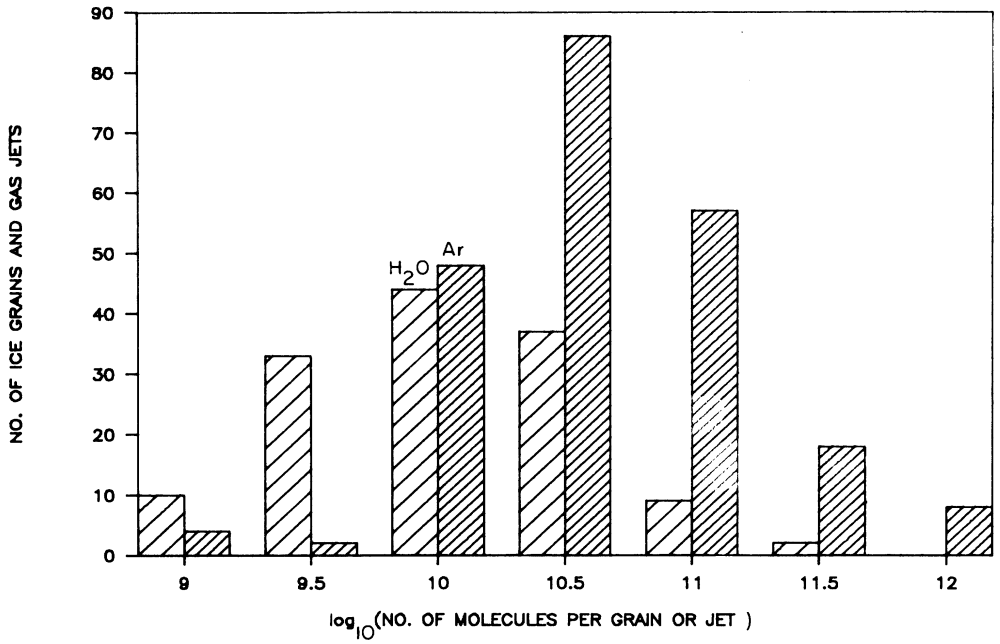

FIG. 4. The distributions of the number of Ar atoms per jet and water molecules per grain. The jets and grains were emitted at 36–39 K, from co-deposition, at 25 K, of 1:1 Ar-H_2O mixtures.

ice needle, with a density of 0.9 g cm^{-3}, as for cubic ice,[8] would result in a needle radius of ~ 0.2 μm and a length of ~ 1 μm. From the trajectories of the ice needles reaching the mass-filter probe, a minimal speed of 167 cm sec^{-1} can be obtained. This speed requires, for a needle containing 10^{10} water molecules, an energy of 4×10^{-9} erg. In a jet of 3×10^{10} argon atoms, at 50 K the available energy (nkT) is 2×10^{-4} erg; sufficient to propel the needles at a speed of 3.6×10^{4} cm sec^{-1}. The mechanism proposed for jet formation and the ejection of ice needles will be discussed later, in Sec. III D.

C. Trapping of Ne, H_2, and D_2

Further insight into the structure of the amorphous ice and the mechanism by which it traps gases was obtained by studying the trapping of smaller atoms and molecules, such as Ne, H_2, and D_2 in ice below 20 K. Three typical plots of the evolution of Ne, H_2, and D_2 from the ice in co-deposition experiments, as a function of temperature, are shown in Fig. 5. Three distinct ranges of gas release are observed for all three gases: 16–35 K, 35–85 K, and 85–120 K. With Ne, an additional, small peak at 137 K (the transition to cubic ice) was also observed. The highest amount of gas trapped in the first range, gives a gas-to-ice ratio as high as 0.42, whereas in the next two ranges, the amounts are typically ~ 6 and ~ 3 times smaller, respectively. Altogether, a gas-to-ice ratio of up to 0.63 (by number) is obtained. Much smaller amounts of these gases are trapped in the ice between 20 and 25 K, neon being the least affected by the higher temperatures.

Brackmann and Fite[3] also observed a sharp rise in the desorption of H_2 from ice at ~ 17 K, but did not report the quantity of adsorbed gas. Govers *et al.*[4] found only a monolayer coverage of H_2 on a condensate of the residual gases (water, air, and hydrocarbons) on a cold ($T \leq 6$ K) substrate. Kahane *et al.*[5] trapped Ne at a gas-to-ice ratio of 1:600 by applying a Ne pressure of 125 bar to hexagonal ice at 248 K.

The second and third ranges of gas release occur at exactly the same temperatures as ranges (*b*) and (*d*) in the previous argon study (Fig. 1) and will therefore be labeled (*b*) and (*d*), accordingly. The coincidence of these two ranges of gas release for Ne, H_2, and D_2 with those for the larger and more polarizable CH_4, CO, N_2, and Ar suggest that they are a result of processes in the ice itself and are not caused by the interactions of the gases with the ice. Since the phase transition of amorphous ice into cubic ice occurs only at 136.8 K, it was suggested[2] that ranges (*b*) and (*d*) are due to two distinct steps of annealing of the amorphous ice, from 35 to 85 K and from 85 to 120 K. The question then arose whether the two annealing processes proceed to completion when the ice is kept at a constant temperature of ~ 50 or ~ 90 K, like the phase transition to cubic ice at 136.8 K: When argon-laden ice is kept at a constant temperature of 140 K for several hours, argon evolves continuously until it is completely exhausted. Further heating of the ice to 150 K does not result in any further gas evolution. Thus the phase transition to cubic ice is completed within several hours, once the transition temperature is reached, and a new surge of gas occurs only at 160 K during the next phase transition to hexagonal ice. A similar experiment was thus performed in range (*b*), where the argon-laden ice sample was kept at 50 K for 16 h. During this period, the gas flow diminished from 10^{14} atoms/sec to the limit of detection—10^{9} atoms/sec.

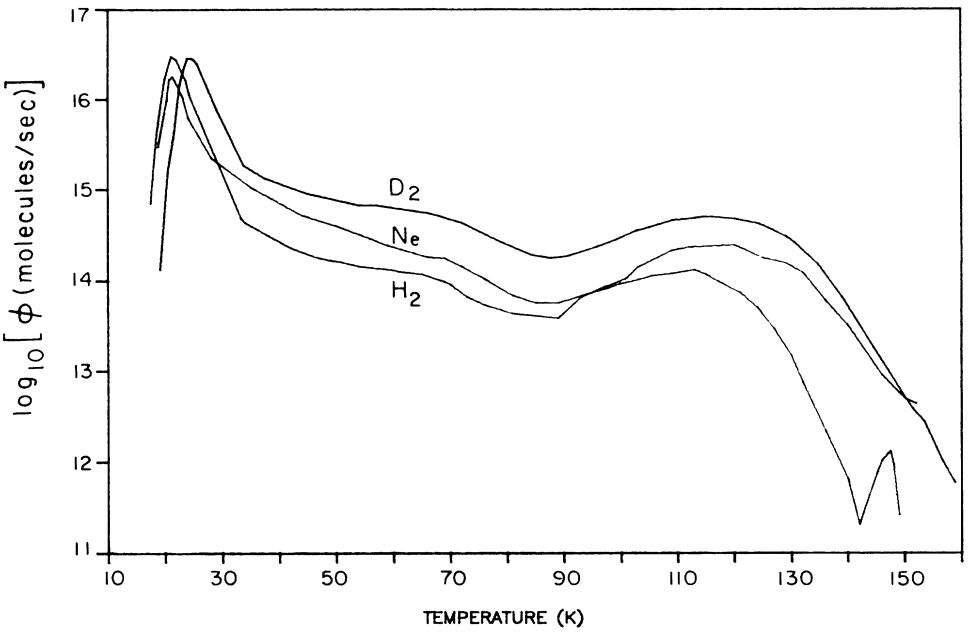

FIG. 5. A plot of the fluxes (ϕ) of evolved H_2, D_2, and Ne vs temperature, from co-deposition, at 16–18 K, of 1:1 gas-H_2O mixtures.

However, when the ice was heated to 55 K, the gas flow was resumed, and reached again a flux of 10^{14} atoms/sec. The same behavior was observed in the second range of annealing (d), with an ice sample which was kept at 90–95 K for 10 h. Heating to a mere 96 K resulted in a sharp rise in the gas flow from 10^9 to 10^{14} atoms/sec. Hydrogen behaves in a similar manner. The conclusion from these three experiments is rather straightforward: Whereas the amorphous ice transforms completely to cubic ice once the transition temperature of 136.8 K is reached, the annealing in ranges (b) and (d) proceeds through a large number of metastable states, each corresponding to a certain temperature, and the ice cannot pass from one state to the next one unless the temperature is raised. Presumably, at each temperature only a certain fraction of the water molecules in the amorphous ice change their position or orientation.

Further insight into the nature of ranges (b) and (d) was obtained by flowing argon, neon, and hydrogen into cubic ice, which was recooled to 19 K. None of these gases evolved in range (d) but, surprisingly, a large amount of neon, very little hydrogen, and no argon were released again in range (b). Range (b) cannot be attributed to the annealing of amorphous ice, since the ice was already in its cubic form. Alternatively, cooling the cubic ice to 19 K cracked it and opened new crevices, large enough for hydrogen and neon, but too small for the argon. Upon warming, these crevices annealed in range (b) and pushed out the trapped neon and hydrogen. However, as will be shown later, most of the hydrogen came out earlier, in range (c). Thus range (b) can be attributed to the annealing of small crevices in amorphous or cubic ice, whereas range (d) is due to the stepwise, irreversible annealing of one form of amorphous ice into another form of amorphous ice. It seems therefore justifiable to define two forms of amorphous ice, each one being stable at a different temperature range: I at $T < 85$ K and II at $85 < T < 136.8$ K. Perhaps a third form, III at $120 < T < 136.8$ K, where peak (d') emerges [Fig. 1(a)], might be associated with the glass transition.[2]

The first range of gas release for neon, hydrogen, and deuterium starts at 16 K. Unlike in the case of argon, this range cannot be attributed to the evaporation of frozen gases—range (a)—since they do not freeze between 16 and 20 K. The nearest range of gas release in the argon study [except (b) and (d)] was range (c) [Fig. 1(a)], which was attributed to the adsorption of a monolayer of argon on the ice surface.[2] Therefore it seems that the first range of gas release in the present study could be due to some sort of adsorption and should also be labeled (c), according to our previous labeling. Additional support to the suggestion of adsorption is lent by the observation that the trapping of the three gases in (c) is reversible. If, after the gas in range (c) is completely released at 25 K, the ice is recooled to 15–19 K and additional gas is flowed into it, a certain amount of trapped gas is restored. With hydrogen, the restoration is within the limits of four times more to ten times less gas than the initial amount; 1–0.03 with D_2 and 1–0.01 with Ne (Fig. 6). The variability in the amount of restored gas does not depend on the exact temperature, between 15 and 19 K, the amount of ice, or the gas pressure. Even if the amorphous ice is transformed to cubic ice (at 143 K) prior to recooling and hydrogen or deuterium flow, the amount of gas trapped in (c) does not vary more than in the samples which were warmed only to 25 K. But, contrary to hydrogen and deuterium, neon is not trapped anymore in range (c) in the cubic ice.

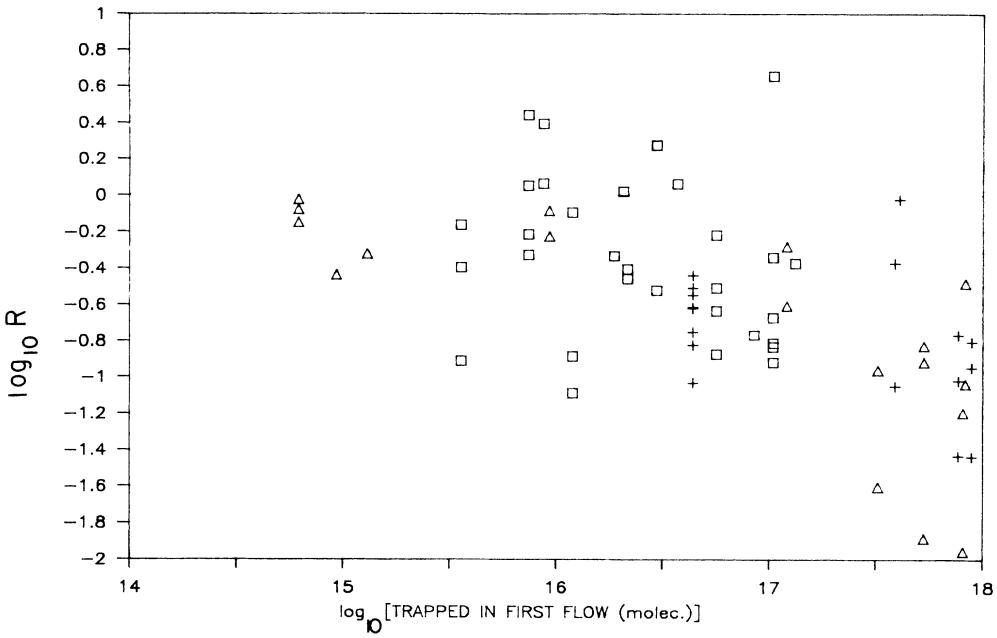

FIG. 6. The ratio (R) of trapped gas in subsequent gas flows into ice, divided by the amount of gas trapped in the first flow (or co-deposition) vs the amount trapped in the first flow. □, H_2; +, D_2; △, Ne.

The most striking finding of these experiments is the trapping of up to 42% of hydrogen, deuterium, and neon in the amorphous ice, in range (c), between 15 and 19 K. The amounts of gas trapped in (b) and (d) are ~6 and ~3 times smaller, respectively. In our previous study,[2] the argon which was adsorbed as a monolayer on the ice surface in range (c) reached a gas-to-ice ratio of only 0.018. Yet even this small ratio gave a surface area of 86 $m^2 g^{-1}$ for the amorphous ice. A ratio of 0.42 would require a surface area larger than 1000 $m^2 g^{-1}$, which is hard to accept; especially so, since warming to 100 K, which reduced the surface area as measured by Ar adsorption to 55 $m^2 g^{-1}$,[2] did not affect the trapping of H_2, D_2, and Ne in range (c). Thus there seems to be no correlation between the surface area, as measured by Ar adsorption, and the capacity for trapping Ne, H_2, and D_2 in range (c). Calculation of a fractal dimension from the 42% Ne and 1.8% Ar which were trapped in range (c) and their diameters—3.8 Å and 4.7 Å, respectively[9,10]—yielded a value much larger than 3. Thus the trapping of so much Ne, H_2, and D_2 is not due to a fractal structure of the ice. In order to trap up to 42% of these gases in range (c), they have to penetrate into the entire amorphous ice lattice. A bulk behavior is suggested also by the increase in the ratio of trapped gas to ice with increasing amount of ice (Fig. 7). The question arises then, how do these gases penetrate the amorphous ice lattice? An answer to this question should explain also the mechanisms by which larger gases, such as argon, are trapped in the ice and why they emerge from the ice in small and large jets rather than continuously.

D. The mechanism of gas trapping and jet formation

According to Hobbs,[8] in cubic ice, the hexagons which are formed by the oxygen atoms have the configuration shown in Fig. 8, with distances of 4.5 and 2.75 Å between adjacent oxygen atoms. With a radius of 1.4 Å for the oxygen atoms,[9,10] the free channel through each hexagon has a diameter of 2.5 Å. The diameters of Ar, Ne, H, and D atoms are 4.7, 3.8, and 2.2 Å, respectively.[9,10] Therefore hydrogen and deuterium molecules, but not neon or argon, can penetrate freely the lattice of cubic ice. Only the amorphous ice lattice, in which the distances between adjacent oxygen atoms are larger,[11] is permeable to neon, and some channels are even large enough to allow argon atoms to penetrate the ice lattice.

This is clearly demonstrated by the reversible trapping in range (c) of H_2 and D_2 in cubic ice, which was cooled to 19 K, and the failure of Ne and Ar to be trapped under these conditions. Yet, considerable amounts of H_2 and D_2 are held in the ice until ranges (b) and (d) are reached, even though the ice matrix is open to them. Apparently, some of the open channels are blocked by domains in the ice which are perpendicular to each other. Hence the amounts of H_2 and D_2 which are emitted in (b) and (d) versus the amount in (c) provide a measure of the fraction of blocked domains in the ice: Of the 0.63 H_2 molecules per water molecule in the ice, 0.42 reside in open channels (c) and 0.21 reside in blocked regions, which open when the ice anneals in ranges (b) and (d). This blocking changes considerably with time and temperature, as demonstrated by the high variability in the amount of trapped gas in subsequent gas flows, into recooled ice samples (Fig. 6).

As for the larger argon atoms, in co-deposition of a gas–water-vapor mixtures, the underlying gas-filled channels are blocked by the added layers of ice, whereas when gas is flowed into preexisting amorphous ice, the channels are blocked by the constant annealing of the ice. The importance of the annealing process was

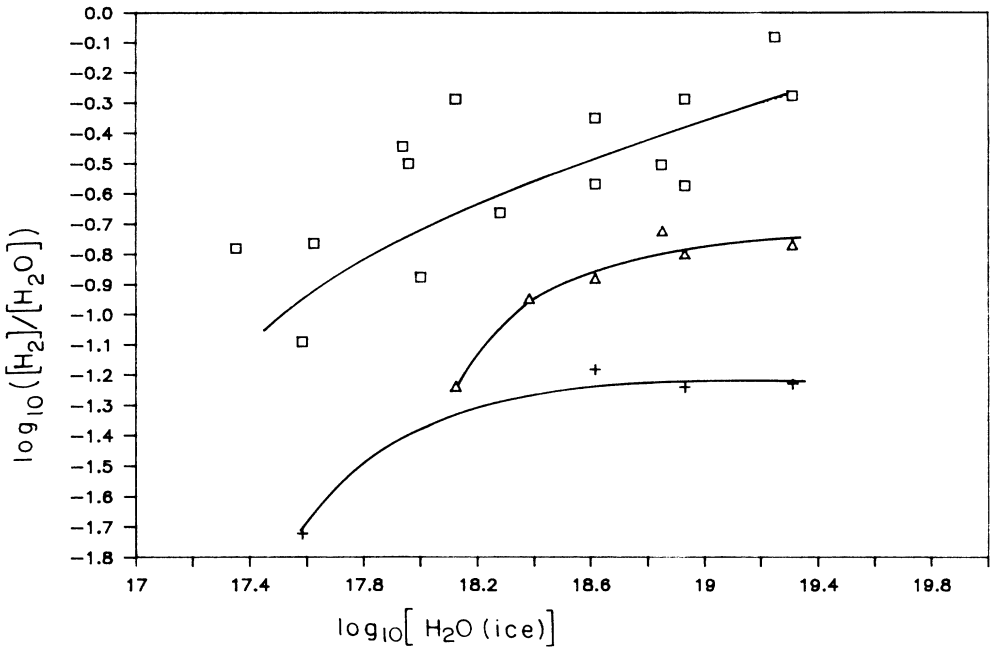

FIG. 7. The amount of trapped H_2 in the three ranges vs the amount of water ice □, range (*c*); +, range (*b*); △, range (*d*).

demonstrated[2] by the sharp reduction in the amount of internally trapped argon when flowed into ice below 25 K, where the annealing and hence channel blocking is very slow.[2] Thus the argon atoms are locked inside the wide channels in the amorphous ice matrix, either completely isolated from each other or in small clusters. Upon warming, when the ice anneals, the rearrangement of the water molecules opens some of the blocked channels. However, only when a channel opens all the way to the ice surface can the gas in it escape out. Thus a dynamic percolation behavior results,[12,13] where only a connection of many gas-filled domains in the ice, up to the surface, forms a minijet. While the larger gases (Ar, CO, CH_4, N_2, and Ne) emerge in minijets, the smaller H_2 and D_2 molecules emerge continuously and reversibly, since the channels in both amorphous and cubic ice are wide enough for them to get through without obstruction.

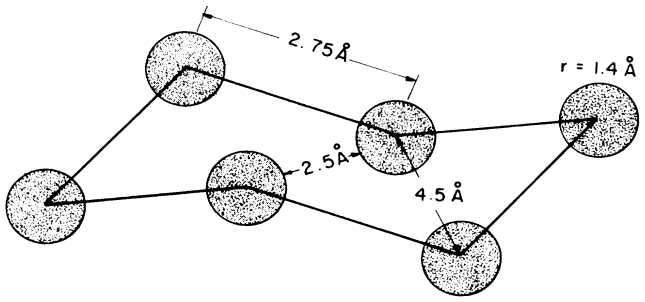

FIG. 8. The configuration of a hexagon of oxygen atoms in a cubic ice lattice (after Ref. 8). Two hydrogen atoms (not shown) are adjacent to each oxygen atom. The diameter of the free channel through the hexagon is 2.5 Å.

The large jets are formed when many small channels open simultaneously, not to the surface, but to a weak region in the ice, where the gases build up a pressure large enough to rupture the overlying ice. This rupture breaks the ice needles from their base and the outflowing gas propels them.

A dynamic percolation behavior can explain also the inflation of the amorphous ice when argon is flowed into it at a pressure exceeding 2.6 dyn cm^{-2}, below 29 K.[2] Each impinging argon atom creates a defect in the ice matrix, which does not anneal fast enough below 29 K. When, at a gas flux corresponding to 2.6 dyn cm^{-2}, the density of unannealed defects surpasses a certain threshold, the ice matrix collapses altogether and a huge amount of gas can be trapped in it, up to a gas-to-ice ratio of 3.3.[2] A similar dynamic percolation behavior was demonstrated experimentally (Blanc and Guyon, in Ref. 12) by applying increasing pressures of mercury onto a porous rock until, above a certain pressure, the rock collapsed and all its internal pores were filled with mercury. A similar system of a random-fuse model for breaking processes was treated mathematically by de Arcangelis *et al.*[14]

IV. CONCLUSIONS AND APPLICATIONS

A deeper insight into the structure and dynamics of amorphous water ice was obtained in this study: Ballistic water-vapor deposition results in the growth of smooth ice needles ~ 1 μm long and ~ 0.2 μm wide, which comprise at lease 80% of the 10^{18}–10^{19} water molecules/cm^2 deposited. The very fluffy structure accounts for the large surface area (86 $m^2 g^{-1}$) of the ice, as measured by Ar adsorption.

The amorphous ice seems to exist in at least two separate forms: at $T < 85$ K and at $85 < T < 136.8$ K,

with perhaps a third one at $120 < T < 136.8$ K. These forms change irreversibly from one to the other through a series of temperature-dependent metastable states. Each change is accompanied by the release of some of the trapped gas from the ice.

The channels which are formed by the water hexagons are wide enough, even in cubic ice, to allow the penetration of up to 63% of H_2 and D_2, but only in amorphous ice are the channels wide enough for Ar, CO, CH_4, and N_2 to squeeze in. The small Ne is an intermediate case. Amorphous ice which was annealed at 120 K behaves already like cubic ice.

The gas-filled channels in the ice are closed by the annealing ice or by additional ice layers. Further annealing or phase transition of the ice connects gas-filled regions, through dynamic percolation, up to the surface and results in gas emission in minijets. Channels which open into internal holes build up a pressure large enough to rupture the overlying ice and propel the $\sim 1 \times 0.2$ μm^2 ice needles by the large gas jets, each containing 10^{10}–10^{11} gas atoms.

Dynamic percolation behavior also explains the collapse of the amorphous ice matrix under a gas pressure of 2.6 dyn cm^{-2}, below 29 K, and the burial of enormous amounts of gas in it.

The experimental findings are readily applicable to icy bodies in the solar system and in dense interstellar clouds. Thus the agglomeration of the fluffy, needlelike ice to form comets could have resulted in cometary nuclei of very low density, in accordance with the density of 0.17 g cm^{-3}, which was recently calculated for comet P/Halley by Rickman.[15]

The experimentally observed accumulation of large quantities of gas in pockets and their occasional explosion, with the propulsion of the ice fragments by gas jets, is also directly applicable to comets: Upon warming by solar radiation, the outer, ~50-m-thick layer of a pristine cometary nucleus, made of gas-rich amorphous ice, would reach 137 K and transform into crystalline ice.[16] A fraction of the gases released from this layer would be trapped in pockets, which would explode occasionally, giving rise to the frequent small bursts which were observed on P/Halley.[17] These explosions would also blow off the accumulated layer of dark cometary dust, which keeps the nucleus well insulated and inactive.[18,19] The exposed ice would sublimate violently and widen the hole until a large crater is formed,[16] like the craters observed by the Giotto and Vega spacecrafts on P/Halley.

Yet another application of the experimental results is the trapping of up to 63% of hydrogen in ice below 20 K. It is expected that the fluffy ice mantles of grains in dense and cold (~10 K) interstellar clouds would be hydrogen-rich. About 21% of the hydrogen would not be lost upon warming to 50 K and 14% not even at 80 K. The possible contributions of this hydrogen to comets will be discussed elsewhere.[20]

ACKNOWLEDGMENTS

We wish to thank D. Bergman, I. Goldberg, and B. Dwir for helpful discussions. This research was supported by the NASA Exobiology Program, through the State University of New York at Stony Brook.

[1]A. Bar-Nun, G. Herman, D. Laufer, and M. L. Rappaport, Icarus **63**, 317 (1985).
[2]A. Bar-Nun, J. Dror, E. Kochavi, and D. Laufer, Phys. Rev. B **35**, 2427 (1987).
[3]R. T. Brackmann and W. L. Fite, J. Chem. Phys. **34**, 1572 (1961).
[4]T. R. Govers, L. Mattera, and G. Scoles, J. Chem. Phys. **27**, 5446 (1980).
[5]A. Kahane, J. Klinger, and M. Phillippe, Solid State Commun. **7**, 1055 (1969).
[6]J. C. Phillips, Physics Today **35** (2), 27 (1982).
[7]P. Meakin, Phys. Rev. B **30**, 4207 (1984).
[8]P. V. Hobbs, *Ice Physics* (Clarendon, Oxford, 1974), pp. 19–60.
[9]L. Pauling, *The Nature of the Chemical Bond,* 3rd ed. (Cornell University Press, Ithaca, 1960).
[10]*CRC Handbook of Chemistry and Physics* (CRC, Boca Raton, Florida, 1982).
[11]W. G. Madden, M. S. Bergren, R. McGraw, S. A. Rice, and M. G. Sceats, J. Chem. Phys. **69**, 3497 (1978).
[12]*Percolation Structures and Processes,* edited by G. Deutcher, R. Zallen, and J. Adler (Hilger, Bristol, and The Israel Physical Society, Jerusalem, 1983).
[13]D. Stauffer, *Introduction to Percolation Theory* (Taylor & Francis, London, 1985).
[14]L. de Arcangelis, S. Redner, and H. J. Herrmann, J. Phys. (Paris) Lett. **46**, L585 (1985).
[15]H. Rickman, in *The Comet Nucleus Sample Return Mission,* Proceedings Workshop, Canterbury, European Space Agency Report No. SP-249, 1986.
[16]D. Prialnik and A. Bar-Nun, Astrophys. J. **313**, 893 (1987).
[17]M. C. Festou, P. D. Feldman, M. F. A'Hearn, C. Arpigny, C. B. Cosmovici, A. C. Danks, L. A. McFadden, R. Gilmozzi, P. Patriarchi, G. P. Tozzi, M. K. Wallis, and H. A. Weaver, Nature **321**, 361 (1986).
[18]H. J. Reitsema, W. F. Heubner, and F. L. Whipple Bull. Am. Astron. Soc. **18**, 791 (1986).
[19]J. M. Lamarre *et al.*, Bull. Am. Astron. Soc. **18**, 794 (1986).
[20]A. Bar-nun and D. Pricelnik, Astrophys. J. Lett. (to be published).

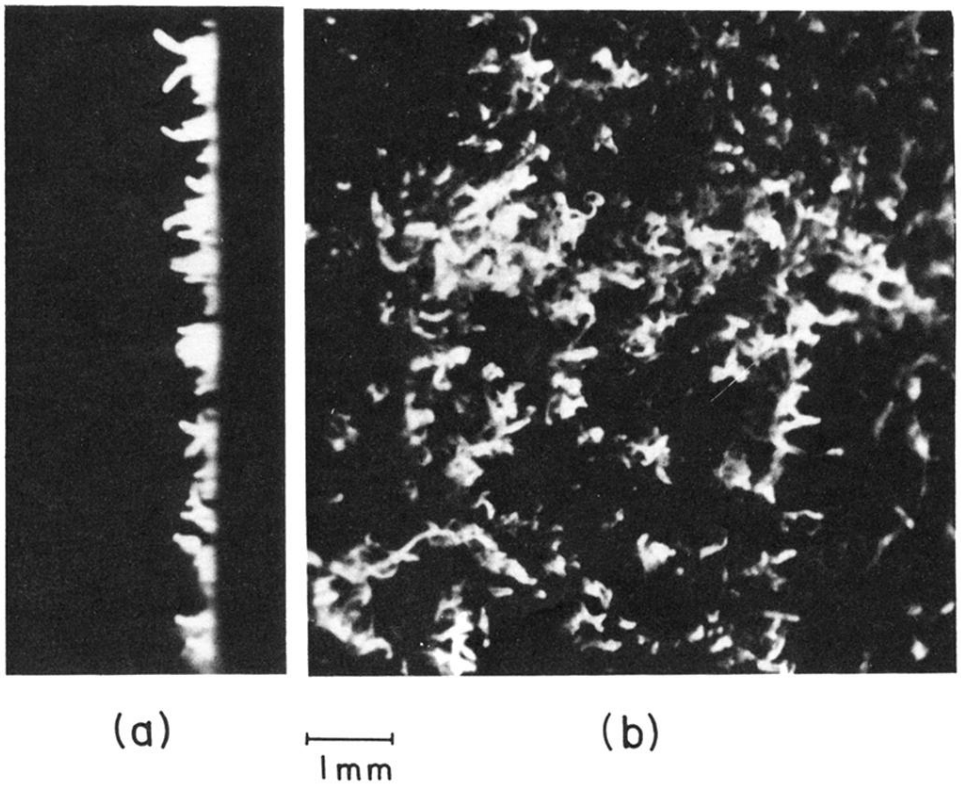

FIG. 2. Two views of an amorphous ice layer, seen edge-on (a) and at an oblique angle (b), both magnified 15 times. Needles about 0.1 mm long are seen, with an ice layer containing $\sim 10^{20}$ water molecules/cm^2.